Nanotechnology Perceptions
ISSN 1660-6795
www.nano-ntp.com

A Novel Wound Dressing: Psyllium Doped Silver Nanoparticles with Human Amniotic Membrane for Wound Healing

K. Dhanalakshmi[1], Raghu Babu Pothireddy[2], Dr. Mary Vergheese T[1*], Iadalin Ryntathiang[3], Mukesh Kumar Dharmalingam Jothinathan[3]

[1]Department of Chemistry, Madras Christian College, East Tambaram, Chennai-59, Tamil Nadu, India.
[2]Acadicell Innovations International Pvt. Ltd., Peerakankaranai, Vandalur, Chennai-600048, Tamil Nadu, India.
[3]Centre for Global Health Research, Saveetha Medical College and Hospitals, Saveetha Institute of Medical and Technical Sciences (SIMATS), Saveetha University, Chennai, India.
Email: maryvergheese@mcc.edu.in

Introduction: Wound healing is a complex process that requires effective interventions to prevent infection and promote tissue regeneration. Recent advances have highlighted the potential of using nanotechnology in wound dressings. In this study, we explore a novel wound dressing composed of psyllium-doped silver nanoparticles (AgNPs) incorporated with human amniotic membrane (HAM). Psyllium, a natural polymer, is known for its biocompatibility and gel-forming properties, while silver nanoparticles offer broad-spectrum antimicrobial activity. The objective of the study is to reduce the effects of wounds by combining the Human Amniotic Membrane (HAM) with silver nitrate-doped Psyllium seed extract (PSE). Materials and methods: For this study, an extract of Psyllium seed husk was obtained and doped with AgNPs. The HAM was also collected and processed. After sterilization, the membrane was combined with the prepared Psyllium AgNPs. The wound dressing was characterized by invitro assays. Characterization of the synthesized Psyllium-AgNPs was performed using various quality control tests. The tensile strength of the processed membrane was also tested. Results: The psyllium-doped AgNPs were successfully synthesized, with TEM images confirming a uniform distribution of nanoparticles. The MTT assay showed no cytotoxicity of the formulated drug, and the scratch assay showed an increase in the percentage of wound closure compared with the control. Conclusion: The novel wound dressing, which incorporates Psyllium-doped AgNPs with HAM, shows promising biocompatibility and efficacy in in vitro wound healing. This novel methodology has the potential to be used in future extensive experiments, verification, and commercialization, providing a fresh alternative for improved wound treatment.

Keywords: Psyllium Seed Extract, Human Amniotic Membrane, Silver Nanoparticles, Wound

healing, Wound dressing.

1. Introduction

Wounds are a challenging clinical issue, with early and late complications causing morbidity and mortality. In general, a wound is defined as disruption of the integrity of the skin, membrane, or tissue. Wounds can be distinguished as simple or complex depending on the region to which are confined. Wound healing is a natural physiological reaction to any tissue injury (Chhabra et al., 2017). The process of wound healing is complex and involves highly coordinated phases like coagulation & hemostasis, inflammation, granulation tissue formation, and remodeling, with scar tissue formation.

Once a wound occurs, the immediate reaction is coagulation and hemostasis, which helps maintain the vascular system intact in such a way that other vital organs function despite the injury. As a next step, a matrix is provided for the invading cells. A balance between endothelial cells, thrombocytes, coagulation, and fibrinolysis regulates hemostasis. Together with these events, the activation of the coagulation cascade takes place via extrinsic and intrinsic pathways that lead to platelet aggregation and formation of clots to limit blood loss (Wilkinson & Hardman, 2020). The inflammatory phase follows next, whereas it establishes an immune barrier against invading microorganisms.

The immune barrier is formed by the activation of the complement cascade, which leads to neutrophil infiltration of the wound site, thereby preventing infections. The invasion of neutrophils happens within 24 to 36 hours and is referred to as the early inflammatory phase. The neutrophil activity gradually changes as the microorganisms are removed and further changes to the late inflammatory phase, i.e., late inflammatory phase wherein the macrophages appear in the wound and continue the process of phagocytosis. These cells act as key regulator and provide an abundant reservoir of growth factors, and various mediators like TGF-alpha, EGF, FGF, collagenase, fibroblasts, endothelial cells etc (Landén et al., 2016). The final stage of this phase is the invasion of lymphocytes which makes way for the next phase, the proliferative phase. The proliferative phase is characterized by the migration of fibroblasts and deposition of newly synthesized extracellular matrix that serve as a replacement for provisional networks composed of fibrin and fibronectin. The stages in the proliferative phase include fibroblasts migration, collagen synthesis, angiogenesis, and granulation tissue formation. As these stages pass by, the final stage in wound healing is the remodeling phase, which responsible for the development of new epithelium and finally the formation of scar tissue (El Ayadi et al., 2020).

Wound healing is an uncomplicated process. If it is disturbed by local factors, such as infections, chronic diseases, and even improper personal hygiene, the phase of wound healing is disturbed, thereby causing chronic wounds (Al-Nadaf et al., 2024). Chronic wounds have become a major research topic in recent years because of their increasing prevalence and occurrence. These wounds generate various health problems, thus decreasing the quality of life and productivity of individuals.

With regard to the above-mentioned context, it is essential to have an appropriate approach for treating the wounds, whereby it facilitates the healing process and can have an important

impact on the final clinical outcome. Many studies have been published on effective wound management, but it remains a challenge. Recent clinical trials suggest the use of modern dressings and skin substitutes (Mirhaj et al., 2022). With the use of skin substitutes, Human Amniotic Membrane (HAM) has various biological properties that are useful in the process of wound healing (Tauzin et al., 2014). The amniotic membrane (AM) is an avascular structure that makes up the inner layer of the placenta, encircling the embryo and forming a sac that has amniotic fluid filled in it (Schmiedova et al., 2021). It is made of three layers: Collagen, Extracellular matrix, and active cell-stem cells. The HAM is said to have regenerative qualities, such as analgesic, reduced scarring, epithelization, and angiogenic effects, together with suppressing fibrosis (El-Heneidy et al., 2016). The process of tissue remodeling is regulated by growth factors, cytokines, chemokines, and other regulatory molecules (Fitriani et al., 2023).

On the other hand, nanotechnology is currently providing various materials and approaches for revolutionizing the medical field. Recently, silver nanoparticles (AgNPs) have attracted for their clinical application because of their potential properties, such as anti-bacterial activity, anti-inflammatory effects, and wound healing efficacy, which can be further used as a wound dressing (Gunasekaran et al., 2011). Due to the huge potential of AgNPs in biomedical applications, researchers are currently studying the physiochemical parameters, whereby it is accepted that AgNPs with a smaller diameter have a superior antimicrobial effect than those with a larger diameter, and the antibacterial effect is higher than their bulk equivalents (Paladini et al., 2019).

Psyllium is a natural, soluble fiber that can form a gel when hydrated (McRorie et al., 2021). Systematic and local drugs and drug release are two major approaches for the prevention and treatment of wound infections. Studies have shown that Psyllium extract has the property to form a hydrogel that helps in the sustained release of drugs and aids in healing process (Patil et al., 2011). Hydrogel-based wound dressing materials also possess advantages like immediate pain control effect, easy replacement and transparency, easy handling, oxygen permeability etc (Boateng et al., 2008).

With these compounds, our study aims to reduce the effects of wounds by integrating the HAM with silver nitrate-doped Psyllium seed extract (PSE). To highlight, the research underwent the synthesis of AgNPs from a natural source – Neem.

2. Materials and Methods

A class 10,000 clean-room facility was used to conduct the experiment. For this study, Psyllium Seed husk, AgNPs, and HAM were used as the major components. For the in-vitro assays, Adult Dermal Fibroblast (ADF) cells were cultured.

2.1. Green Synthesis of Silver Nitrate particles

20 grams of neem leaves were measured, washed thoroughly with distilled water, and air-dried. The dried leaves are cut, mixed with distilled water, and heated to 70°C. The cooled and filtered solution is then used for nanoparticle synthesis. Leaf extract was added to silver nitrate solution under continuous magnetic stirring. The color change of the solution from pale yellow to dark brown indicates the formation of AgNPs.

2.2. Extraction of PSE polymer and doping with silver nitrate nanoparticles

The dried psyllium husk was ground in mortar and pestle for size reduction, and the powder was mixed with double distilled water to make a slurry. The slurry was poured and boiled using double distilled water to ensure uniform mixing and was kept overnight. Later, the supernatant was separated by centrifugation, and the residue was washed using petroleum ether, diethyl ether, and acetone.

As a next step, the precipitate was dried at 50-60 °C under vacuum to remove moisture and volatile matter. The required quantity of dried PSE was mixed with silver nitrate ($AgNO_3$) in the dark conditions until the solution turned yellowish brown. The resulting solution was further centrifuged, washed three thrice and stored in a desiccator. Finally, the sample is sieved to obtain particles with uniform size that can be used in characterization studies and wound dressing (Patil et al., 2011).

2.3. Collection and Processing of the HAM

The following research was carried out with the approval of the ethics review committee - The Amnion Membrane were collected from the placental membrane during C-section delivery to reduce contamination and is transferred to sample preservation medium containing antibiotics. For processing, the membrane is placed into a tray filled with distilled water, rinsed, and gently massaged to remove blood stains and blood clots. The membrane was washed with NaCl solution and distilled water to remove salts and fine blood particles. As a final step, excess water is removed from the membrane, placed on a Tyvek pouch, and kept for complete drying in a hot air oven at 40 °C, and then sterilized by Gamma sterilization at a dose of 25kGy.

2.4. Structural Analysis using Fourier Transform Infrared Spectroscopy (FTIR)

Fourier transform infrared (FTIR) (Randolph, MA, USA) spectra of PSE samples were recorded on a Perkin Elmer UATR two instrument between the ranges 400–4000 cm^{-1} by ATR/FTIR.

2.5. Nuclear Magnetic Resonance spectra of PSE

The ^{1}H-NMR studies for PSE were carried out to confirm the presence of carbohydrates and polysaccharides. Distinct peaks in the NMR spectrum provide information about the atoms in a molecule, enabling structure elucidation. A 5 mg vacuum dried PSE sample at 70ºC for 24hrs was prepared in 0.7ml of D^2O and sonicated at 60ºC for 30 mins. The peak assignments were based on literature reports and theoretical values.

2.6. TGA Analysis

Changes in the mass of a sample over time during temperature changes can be analyzed using Thermo Gravimetric Analysis or Thermal Gravimetric Analysis (TGA). TGA was performed for the PSE samples using STA 449 F3 Jupiter (Netzsch, Germany) thermal analyzer carried between 30-600°C using an aluminum pan at a heating rate of 10 K/min under a nitrogen atmosphere with the flow rate of 80 ml/min.

2.7. Particle Size Analysis

In this study, the wt.% sample solution was swelled for 12 h, sonicated for 30 min, and the collected supernatant solution was collected for analysis.

2.8. Detection of tensile strength

The detection process uses a Universal testing machine wherein the product of interest here, the AM is made into a dumbbell of length 3 cm using a dumbbell cutting press to determine the strength and deformation behavior of the membrane.

2.9. MTT Assay

The MTT assay was performed to analyze the toxicity of the developed polymer. For this test, ADF were passaged after reaching 70-80% confluency and cultured in 96-well culture plates. The developed polymer and AgNPs of various concentrations were added to the test wells in triplicate, along with the control and blank. After incubation, MTT reagent was added to a final concentration of 10% and later added to the solubilization solution. The plate was incubated overnight, and absorbance was measured using ELISA reader at 570-600nm wavelength.

2.10. Scratch Assay

The scratch assay was performed to measure the property of cell migration when a scratch (wound) is created by using a pipette tip. The cultured ADF cells were added to a 12-well culture plate, and the test wells were added with the developed product. In this study, the testing products were Amnion Membrane powder, and Psyllium powder, our developed polymer, along with controls. Observation of the plate were taken at 0^{th} hour and 18^{th} hour and distance of the scratch was analyzed using ImageJ software.

2.11. Total Protein Estimation using Bradford Assay

The total protein content in the Dehydrated HAM was quantified using Coomassie reagent, and the protein concentration was calculated from the absorbance value measured at 595nm.

2.12. Cytokine Study using ELISA

The principle applied to the kit is based on the Sandwich enzyme immunoassay. Using at cytokine analysis kit, quantitative analysis of proteins present in the HAM is performed. The concentrations of TGF B1, VEGF A, EGF, bFGF, and PDGF BB were quantified. The enzyme-substrate reaction was measured using an ELISA reader in wavelength range of 450 ± 10 nm. The statistical analysis was performed using OriginPro software.

2.13. H&E staining of HAM

The unprocessed placental membranes were cut into appropriate size and were fixed in 10% (v/v) neutral buffered formalin, dehydrated and them embedded in paraffin wax. Tissue sections were stained with hematoxylin and eosin (H&E) and Masson's trichome and analyzed under a light microscope.

3. Results

3.1. Structural analysis of FTIR

The results of FTIR analysis of the PSE and AgNPs-doped Psyllium extract are shown in Fig 1. The Characteristic peak at a range of 3600-3100 cm^{-1} is due to the stretching vibration of -OH groups, and the sharp peak at 2920 cm^{-1} is attributed to the stretching vibration of -CH groups (Devaraj et al., 2013). The presence of -CO groups showed peaks at 1635 cm^{-1}, ether linkages of the polysaccharides were observed at 1385 cm^{-1} and a peak at 1035 cm^{-1} is due to the stretching vibrations of the cyclic ethers present in PSE. The FTIR spectra of AgNPs-doped Psyllium extract exhibited a prominent shift in peaks between 2920 cm^{-1} to 2929 cm^{-1} and 1635 cm^{-1} to 1644 $cm^{-1,}$ thus confirming the same.

Figure 1: FTIR spectra of PSE and PSE -$AgNO_3$ [PSE-AgNp]

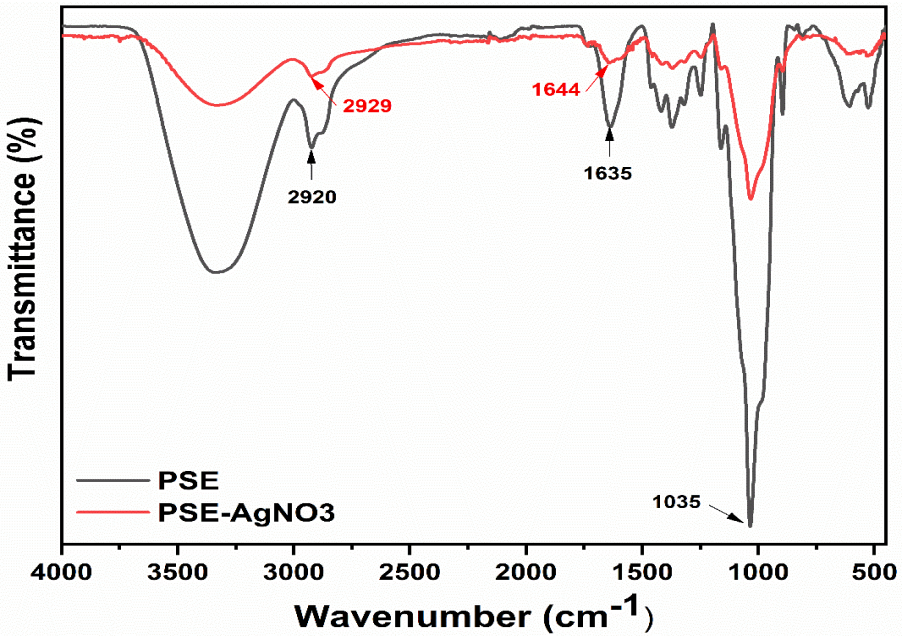

3.2. Nuclear Magnetic Resonance spectra of PSE

The result of the ^{1}H-NMR study is depicted in Fig. 2. The peak at 1.8 ppm can be ascribed to the protons of -CH_2 group. The single peak observed between 3.5-4.0 ppm is attributed to the methane protons of PSE. The spectrum below exhibited typical peaks of protons on the psyllium chain. The peak at 8.21 ppm represents the -OH groups that are present in the system (https://www.ucl.ac.uk/nmr/sites/nmr/files/L2_3_web.pdf, 2024).

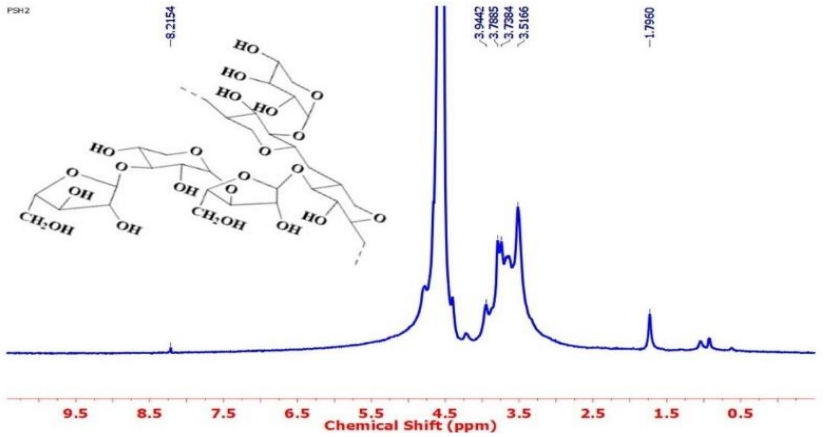

Figure 2: ^{1}H-NMR spectrum showing the structure of the PSE

3.3. UV-Visible spectra of PSE and $AgNO_3$ doped Psyllium extract

The absorption spectra of pure PSE and Psyllium extract doped with AgNPs are shown in Fig. 3. The absorption peak at a wavelength of 276 nm was observed pure PSE. This peak is attributed to the π-π* transition due to the presence of carbonyl groups (C=O) (Rabchinskii et al., 2016). A broadened peak shift at 254 nm was observed for AgNPs doped Psyllium. The blue shift in the spectra between wavelengths 276 – 254 nm is due to the interaction of silver particles with PSE thus confirming the successful doping of silver in the system.

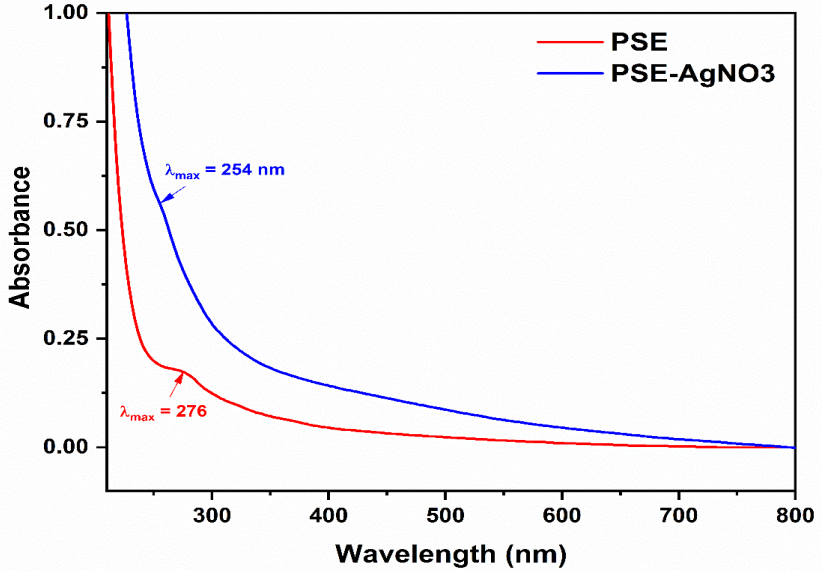

Figure 3: UV-Visible spectra comparing the absorbance between PSE and AG-doped PSE, thus confirming the presence of Ag in the sample

3.4. X-Ray diffraction Method

The results of the X-Ray diffraction study of PSE and PSE-$AgNO_3$ is depicted are depicted in Fig 4 given below. The XRD curves of PSE and PSE-$AgNO_3$ show characteristic peaks at 2 θ = 19.20° and 2 θ = 25.54°, respectively. Also, the peak observed for PSE at 2 θ = 19.20° became weak in the PSE-$AgNO_3$ derivative.

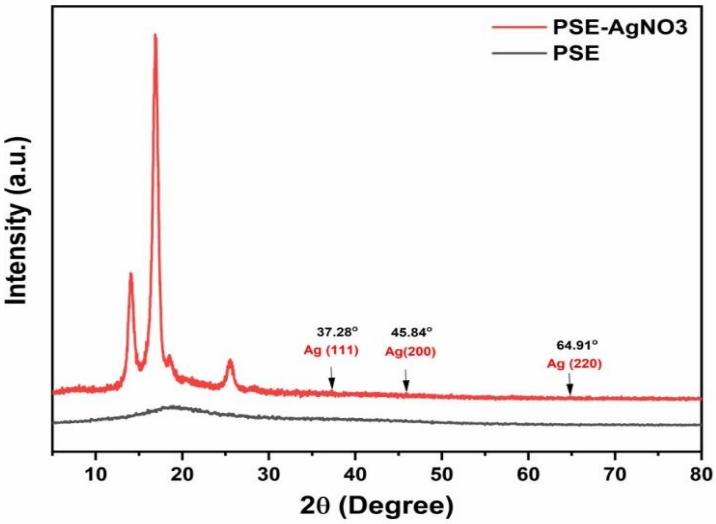

Figure 4: X-Ray diffraction curves of PSE and PSE-$AgNO_3$

3.5. Electron Paramagnetic Analysis (EPR)

The EPR results confirmed the magnetic behavior of the silver particles in the synthesized PSE-Ag polymer, as shown in Fig. 5. In comparing PSE and PSE-$AgNO_3$, the low intensity signal of g=2.0031 is seen in PSE-$AgNO_3$ and no signal was observed in the case of PSE (Khutsishvili et al., 2011).

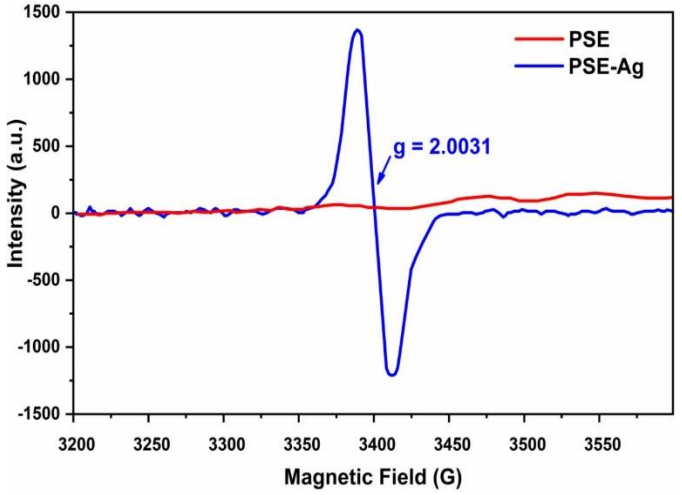

Figure 5: EPR spectra showing the Ag-ions and their magnetic behavior

3.6. Thermogravimetric Analysis (TGA)

The TGA spectra, Fig. 6, depicts the thermal property of PSE, wherein three degradation steps are observed from the studies: 1st degradation shown between 30 to 140 ºC for 5% is due to the removal of moisture, followed by 2nd and 3rd degradation at 280 ºC and 325 ºC respectively. The major decomposition was found to occur between 280 – 310 ºC where the mass obtained was about 34%.

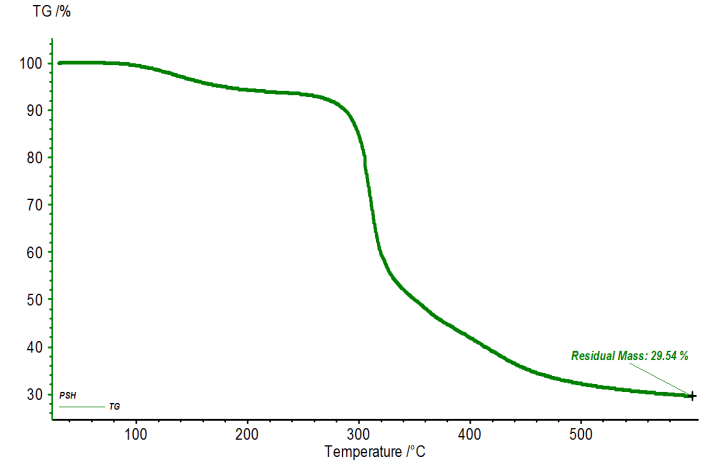

Figure 6: TGA spectra showing PSE decomposition at different temperatures

3.7. Differential Scanning Calorimetry (DSC) Analysis

The results of DSC as depicted in Fig. 7, showed a broad melting point of PSE at around 81ºC and an endothermic broader melting peak at 80 ºC. The broad melting point peaks indicated the non-crystalline nature and stability of the extract against heat (Küçüktürkmen & Bozkır, 2019). The sharp peak at around 300 ºC indicates the endothermic reaction due to the degradation of molecules.

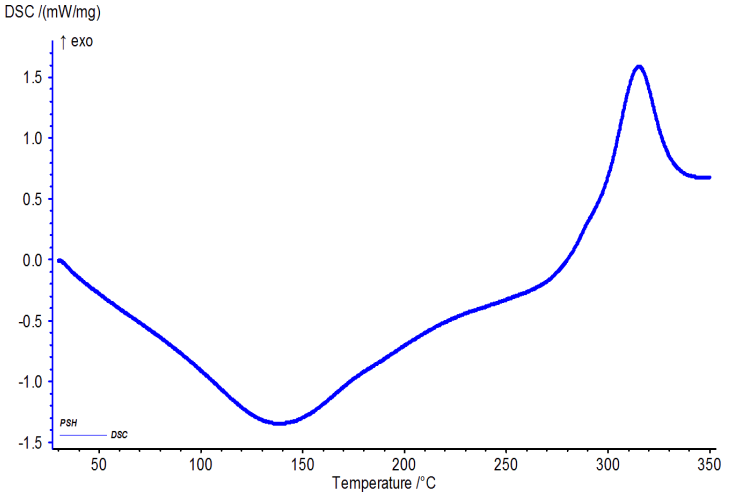

Figure 7: DSC Spectra showing the broad melting point of the PSE

3.8. Particle Size Analysis

The particle size of the 1 wt.% dispersions of extracted PSE in water is shown in Fig. 8. The particle size observed from the analysis was 3940nm.

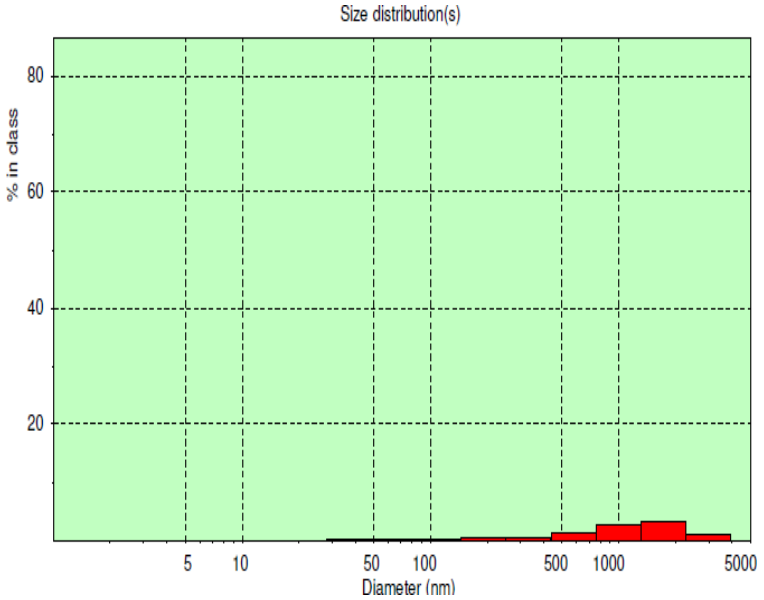

Figure 8: Results of Particle size analysis of the compound PSE

3.9. Transmission Electron Microscopy (TEM) of PSE and PSE-$AgNO_3$

Fig. 9 shows the well distributed AgNPs on the surface of the polymer with size ratio of <10nm. The TEM micrograph shows that the surface is plain, confirming the doping of Ag ions on the surface. The polymer acts as a protective agent, preventing particle agglomeration. The metals were reduced, and uniform distribution of ions on the polymer matrix was observed.

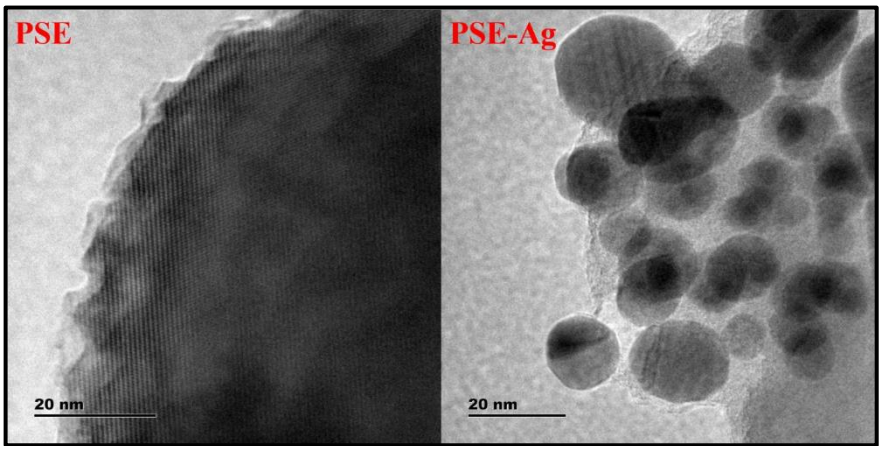

Figure 9: TEM images of PSE and PSE doped with silver nitrate nanoparticles

3.10. Detection of Tensile Strength

The width and thickness of the membrane used for analysis were 3 and 0.036 mm, respectively. Fig. 10 shows the stress-strain graph for the HAM, wherein the observed results are as follows: The Force given at the breaking point of the membrane was found to be 2.411 N, and displacement at Auto break was found to be 11.660 mm; the Elongation of the membrane at the breaking point was 46.640 %. The tensile Strength of the HAM was found to be 22.322 MPa.

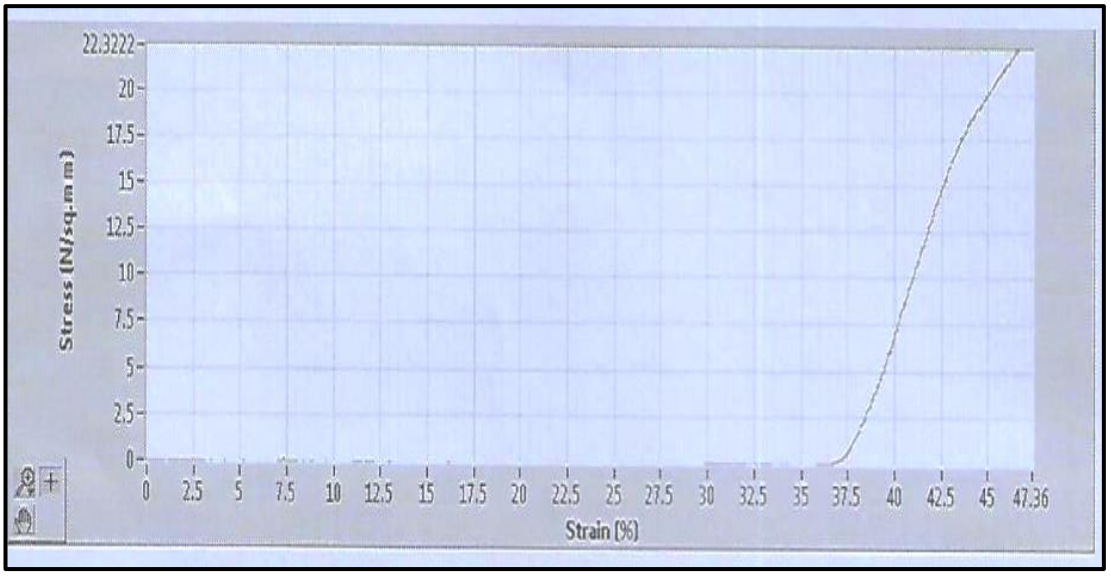

Figure 10: Stress-Strain graph for the dehydrated HAM

3.11. MTT Assay

For this study, each concentration was evaluated in triplicate. 7 test wells were used to measure the cytotoxicity of the (AgNPs). 5 wells were used to measure the cytotoxicity of Amnion powder, and the remaining 5 wells were used for Psyllium powder cytotoxicity testing. The fixed concentration of the compound is based on the high percentage cell survival value and is depicted in Table 1.

Table 1: Considered Concentration Range and Fixed Concentration along with cell survival

Compounds	Concentration Range	Fixed Concentration	% of Cell survival
Amnion Powder	0.5-4mg	2 mg	91.11 %
Psyllium Powder	0.5- 4mg	1 mg	89.24 %
AgNPs	2.5 µg to 25 µg	10 µg	92.85 %

3.12. Scratch Assay

Fixed concentrations that showed optimal cell survival % in the MTT assay were used for the scratch assay to assess the wound healing capacity in vitro. Table 2 depicts, the wound length at 0^{th} and 18^{th} hour. It was observed that after the 18^{th} hour the wound (scratch) was completely closed.

The wound closure percentage was calculated using the formula:

$$\% \text{ of Wound Closure} = \frac{(\text{Initial Scratch wound measurement} - \text{Scratch wound measurement at time X})}{\text{Initial Scratch Wound measurement}} * 100$$

Table 2: Results of Scratch Assay – % of wound closure

Sample	0^{th} hour (mm)	18^{th} hour (mm)	% of Wound Closure
Negative control	0.972	0.793	18.41 %
Positive control	1.060	0.586	44.71 %
Amniotic Membrane	0.920	0.234	74.56 %
Psyllium Powder	0.950	0.377	60.31 %
Developed Wound dressing polymer	1.114	0.232	79.17 %

Comparing the different % values of wound closure in various compounds, it can be observed that the formulated wound dressing polymer, i.e., Psyllium with AgNPs combined with HAM, heals the wounds at a higher rate.

3.13. Total Protein Estimation using Bradford Assay

We observed a change in color of the Coomassie reagent from brown to blue, thereby confirming the presence of protein in the Amniotic membrane. We also measured the protein concentration in the amnion membrane alone and in the entire of the AM (both the amnion and chorion layers together) and found values of 27.19 mg/ml and 39.47 mg/ml, respectively.

3.14. Cytokine Study using ELISA

Because the protein concentration in the AM was high, a thorough cytokine study was performed for both membranes and the concentrations of TGF B1, VEGF A, EGF, b FGF, and PDGF BB were quantified, as shown in Figure 11.

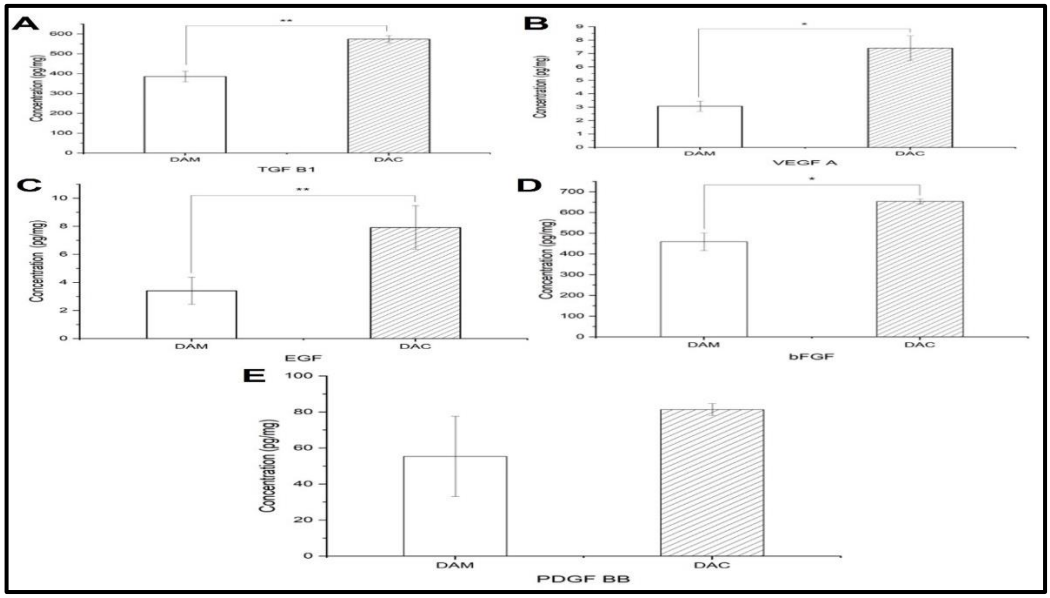

Figure 11: DAM–Dehydrated Amnion Membrane; DAC–Dehydrated Amnion Chorion

Membrane (Amniotic Membrane) (A), (B), (C), (D), and (E) show the different concentrations of various cytokines like TGF B1, VEGF A, EGF, b FGF, and PDGF BB respectively. Statistical significance is denoted by * and * - indicates $p<0.05$ and ** - indicates $p<0.1$.

Cytokine analysis showed higher concentrations in the AM compared to the amnion membrane. Statistically significant results were obtained for TGF B1, VEGF A, EGF. and b FGF.

3.15. H&E staining

The distinguished layers of freshly collected and processed dehydrated amniotic membranes by H&E staining as shown in fig. 12 clearly shows, the amnion and chorion layers. The image also shows that the AM is composed of a single layer of flattened cuboidal cells that rest on the basal lamina as observed (Weidinger et al., 2021).

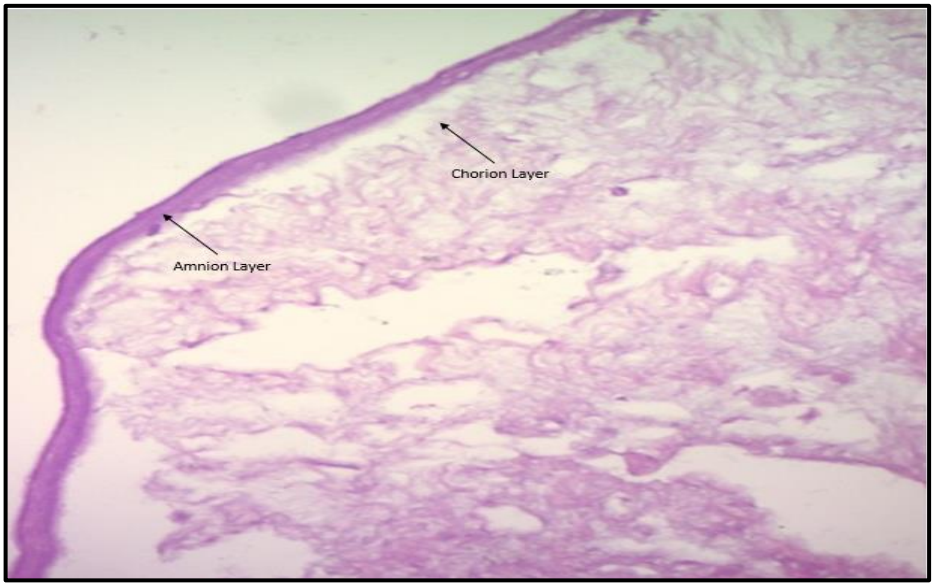

Figure 12: H&E-stained image of the Amniotic Membrane

4. Discussion

Wounds have been prominent pathologies since the beginning of humans, and the medical field has shown drastic improvements in healing in the last few decades. Although it may never be possible to eliminate the risk of wounds that one encounters daily, wound care and management is of major importance, and research tends to expand methods for wound management. The aim of our study was to focus on wound care and management; thus, we developed a wound dressing combining HAM, PSE, and AgNPs.

HAM have biological properties suitable for the purpose of wound healing, and clinical studies have demonstrated its usefulness (Gujjar et al., 2023; Ruiz-Cañada et al., 2021). Briefly, the findings of this study presented the wound healing effects of AM grafts. From Fig.11, the

wound healing effect of the AM was verified via quantitative study of cytokines. Higher values of overall protein concentration are found in the Amnion-Chorion (Amniotic Membrane) and among these, cytokines and growth factors aid in the process of wound healing; observed and suggested by earlier studies. The tensile strength of the AM in our study was found to be 22.32 MPa, and the elongation at break was found to be 46.64%, which is in par with a previous study (Elkhenany et al., 2022; Gremare et al., 2019) that state the AM is highly deformable yet strong and withstands progressive stretching.

In addition, the major effects of the other compounds that were used for the study have been proven. Research suggests that green synthesized silver nitrate nanoparticles show promising results as antibacterial, antimicrobial, and wound healing agents (Ehtesabi et al., 2023). This is in line with our study, which the nanoparticles synthesized from neem showed efficient results in cytotoxicity assay, with a cell survival rate of 92.85%. From Fig.5, the characteristic peak is a confirmation of the magnetic behavior and the formation of free radicals, which correlates with the results of the study (Kim et al., 2007), stating that the antimicrobial property of AgNPs can be due to the formation of free radicals from the surface of Ag. On the other hand, Psyllium extract has demonstrated demulcent and anti-inflammatory activity and is suspected to have wound healing properties (Singh et al., 2011). This was confirmed by the in vitro studies – MTT and scratch assay, whereby the cell survival rate was found to be 89.24 % and 60.31%, respectively. The results of the XRD study suggest that PSE is compatible and leads to the formation of a composite. The pattern obtained for the PSE-$AgNO_3$ derivative in the XRD study suggests that the material displays an amorphous form that can be used in biomedical applications (Ghodke et al., 2021).

Psyllium gel is said to possess antibacterial and enhanced wound healing effects when combined with nanoparticles (Bokaeian et al., 2015). Additionally, the swelling and gelatinous property of psyllium make it a suitable material for drug delivery systems (Masood et al., 2017). In our study, green synthesized AgNPs were doped with PSE and combined with amniotic membrane. Successful doping was confirmed by the characteristic peak observed in the FTIR spectra between 3600-3100 cm^{-1} that aligns with the presence of Psyllium and the blue-shift in the UV-Visible spectra (Ramasamy et al., 2012). The TGA spectra (Fig. 6) and DSC spectra (Fig. 7), showed, a two-stage decomposition behavior as studied (Iqbal et al., 2011) and the third-stage decomposition was due to breakdown of all structural domains. Fig. 9, clearly shows the uniform distribution of AgNPs and the particle size was 20nm, confirming the previously obtained results (Rautela & Rani, 2019).

Combining the effects of the different compounds, the formulated wound dressing in our study showed positive results, eliminating the limitations (Monika et al., 2022) and a higher wound closure percentage of 75.37% in vitro in our study compared with other cases present in the study.

5. Conclusion

Routine preparation and preservation of AM grafts are great value in the future tissue repair programs and biotherapy implementations. The above results tend to prove the various parameters of the compounds used in the study. The formulated wound dressing, i.e., HAM

integrated with AgNPs doped PSE was proved to be biocompatible, and its usage showed promising results in in vitro studies and thus can be concluded to treat wounds. In the future, the dressing could be used in large-scale controlled trials with extended follow-up protocols, further validated, and commercialized as well.

Declaration of interest

The authors declare that they have no known competing financial interests or personal relationships that could have appeared to influence the work reported in this paper.

Funding

This research did not receive any specific grant from any funding agency in the public, commercial or not-for-profit sector.

Author contribution statement

KD: Conceptualization, Data curation, Formal analysis, Investigation, Methodology, Validation, Visualization, Writing - original draft, and Writing - review & editing. RBP: Conceptualization, Data curation, Formal analysis; Investigation, Methodology, Validation, Visualization, Writing - original draft, and Writing - review & editing. MV: Conceptualization, Data curation, Formal analysis; Investigation, Methodology, Validation, Visualization, Writing - original draft, and Writing - review & editing. IR: Conceptualization, Data curation, Formal analysis; Investigation, Methodology, Validation, Visualization, Writing - original draft, and Writing - review & editing. MKDJ: Conceptualization, Data curation, Formal analysis; Investigation, Methodology, Validation, Visualization, Writing - original draft, and Writing - review & editing.

References

1. Chhabra, S., Chhabra, N., Kaur, A., & Gupta, N. (2017). Wound healing concepts in clinical practice of OMFS. Journal of maxillofacial and oral surgery, 16, 403-423. https://doi.org/10.1007/s12663-016-0880-z.
2. Wilkinson, H. N., & Hardman, M. J. (2020). Wound healing: cellular mechanisms and pathological outcomes. Open biology, 10(9), 200223. https://doi.org/10.1098/rsob.200223
3. Landén, N.X., Li, D. & Ståhle, M. (2016). Transition from inflammation to proliferation: a critical step during wound healing. Cellular and Molecular Life Sciences, 73, 3861–3885. https://doi.org/10.1007/s00018-016-2268-0.
4. El Ayadi, A., Jay, J. W., & Prasai, A. (2020). Current approaches targeting the wound healing phases to attenuate fibrosis and scarring. International journal of molecular sciences, 21(3), 1105. https://doi.org/10.3390/ijms21031105.
5. Al-Nadaf, A. H., Awadallah, A., & Thiab, S. (2024). Superior rat wound-healing activity of green synthesized silver nanoparticles from acetonitrile extract of Juglans regia L: Pellicle and leaves. Heliyon, 10(2), e24473. https://doi.org/10.1016/j.heliyon.2024.e24473
6. Mirhaj, M., Labbaf, S., Tavakoli, M., & Seifalian, A. M. (2022). Emerging treatment strategies in wound care. International Wound Journal, 19(7), 1934-1954. https://doi.org/10.1111/iwj.13786.
7. Tauzin, H., Rolin, G., Viennet, C., Saas, P., Humbert, P., & Muret, P. (2014). A skin substitute based on human amniotic membrane. Cell and tissue banking, 15, 257-265.

https://doi.org/10.1007/s10561-014-9427-z.

8. Schmiedova, I., Dembickaja, A., Kiselakova, L., Nowakova, B., & Slama, P. (2021). Using of amniotic membrane derivatives for the treatment of chronic wounds. Membranes, 11(12), 941. https://doi.org/10.3390/membranes11120941.
9. ElHeneidy, H., Omran, E., Halwagy, A., Al-Inany, H., Al-Ansary, M., & Gad, A. (2016). Amniotic membrane can be a valid source for wound healing. International journal of Women's Health, 225-231. https://doi.org/10.2147/IJWH.S96636.
10. Fitriani, N., Wilar, G., Narsa, A. C., Mohammed, A. F., & Wathoni, N. (2023). Application of amniotic membrane in skin regeneration. Pharmaceutics, 15(3), 748. https://doi.org/10.3390/pharmaceutics15030748.
11. Gunasekaran, T., Nigusse, T., & Dhanaraju, M. D. (2011). Silver nanoparticles as real topical bullets for wound healing. Journal of the American college of clinical wound specialists, 3(4), 82-96. https://doi.org/10.1016/j.jcws.2012.05.001.
12. Paladini, F., & Pollini, M. (2019). Antimicrobial silver nanoparticles for wound healing application: progress and future trends. Materials, 12(16), 2540. https://doi.org/10.3390/ma12162540.
13. McRorie Jr, J. W., Gibb, R. D., Sloan, K. J., & McKeown, N. M. (2021). Psyllium: the gel-forming nonfermented isolated fiber that delivers multiple fiber-related health benefits. Nutrition Today, 56(4), 169-182. https://doi.org/10.1097/NT.0000000000000489.
14. Patil, B. S., Mastiholimath, V. S., & Kulkarni, A. R. (2011). Development and evaluation of psyllium seed husk polysaccharide based wound dressing films. Oriental pharmacy and experimental medicine, 11, 123-129. https://doi.org/10.1007/s13596-011-0012-8.
15. Boateng, J. S., Matthews, K. H., Stevens, H. N., & Eccleston, G. M. (2008). Wound healing dressings and drug delivery systems: a review. Journal of pharmaceutical sciences, 97(8), 2892-2923. https://doi.org/10.1002/jps.21210.
16. Devaraj, P., Kumari, P., Aarti, C., & Renganathan, A. (2013). Synthesis and characterization of silver nanoparticles using cannonball leaves and their cytotoxic activity against MCF-7 cell line. Journal of nanotechnology, 2013(1), 598328. https://doi.org/10.1155/2013/598328.
17. NMR Chemical Shifts n.d. https://www.ucl.ac.uk/nmr/sites/nmr/files/L2_3_web.pdf (accessed February 13, 2024).
18. Rabchinskii, M. K., Shnitov, V. V., Dideikin, A. T., Aleksenskii, A. E., Vul', S. P., Baidakova, M. V., ... & Molodtsov, S. L. (2016). Nanoscale perforation of graphene oxide during photoreduction process in the argon atmosphere. The Journal of Physical Chemistry C, 120(49), 28261-28269. https://doi.org/10.1021/acs.jpcc.6b08758.
19. Khutsishvili, S. S., Vakul'Skaya, T. I., Kuznetsova, N. P., Ermakova, T. G., & Pozdnyakov, A. S. (2011). EPR investigation of nanosized silver particles in polymer composites. Magnetic Resonance in Solids. Electronic Journal, 13(1), 1-4.
20. Küçüktürkmen, B., & Bozkır, A. (2019). A new approach for drug targeting to the central nervous system: Lipid nanoparticles. In Nanoarchitectonics in Biomedicine (pp. 335-369). William Andrew Publishing. https://doi.org/10.1016/B978-0-12-816200-2.00014-1
21. Weidinger, A., Poženel, L., Wolbank, S., & Banerjee, A. (2021). Sub-regional differences of the human amniotic membrane and their potential impact on tissue regeneration application. Frontiers in Bioengineering and Biotechnology, 8, 613804. https://doi.org/10.3389/fbioe.2020.613804.
22. Gujjar, S., Venkataprasanna, K. S., Tiwari, S., Sharma, J. C., Sharma, P., Pujani, M., ... & Mathapati, S. (2023). Stabilized human amniotic membrane for enhanced sustainability and biocompatibility. Process Biochemistry, 129, 67-75. https://doi.org/10.1016/j.procbio.2023.03.009.
23. Ruiz-Cañada, C., Bernabé-García, Á., Liarte, S., Rodríguez-Valiente, M., & Nicolás, F. J. (2021). Chronic wound healing by amniotic membrane: TGF-β and EGF signaling modulation

in re-epithelialization. Frontiers in Bioengineering and Biotechnology, 9, 689328. https://doi.org/10.3389/fbioe.2021.689328.

24. Elkhenany, H., El-Derby, A., Abd Elkodous, M., Salah, R. A., Lotfy, A., & El-Badri, N. (2022). Applications of the amniotic membrane in tissue engineering and regeneration: the hundred-year challenge. Stem Cell Research & Therapy, 13, 1-19. https://doi.org/10.1186/s13287-021-02684-0.
25. Gremare, A., Jean-Gilles, S., Musqui, P., Magnan, L., Torres, Y., Fenelon, M., ... & L'heureux, N. (2019). Cartography of the mechanical properties of the human amniotic membrane. Journal of the mechanical behavior of biomedical materials, 99, 18-26. https://doi.org/10.1016/j.jmbbm.2019.07.007
26. Ehtesabi, H., Fayaz, M., Hosseini-Doabi, F., & Rezaei, P. (2023). The application of green synthesis nanoparticles in wound healing: a review. Materials Today Sustainability, 21, 100272. https://doi.org/10.1016/j.mtsust.2022.100272.
27. Kim, J. S., Kuk, E., Yu, K. N., Kim, J. H., Park, S. J., Lee, H. J., ... & Cho, M. H. (2007). Antimicrobial effects of silver nanoparticles. Nanomedicine: Nanotechnology, biology and medicine, 3(1), 95-101. https://doi.org/10.1016/j.nano.2006.12.001.
28. Singh, S., Singh, R., Kumar, N., & Kumar, R. (2011). Wound healing activity of ethanolic extract of Plantago Ovata (Ispaghula) seeds. Journal of Applied Pharmaceutical Science, 1(7), 108-111.
29. Ghodke, S. A., Maheshwari, U., Gupta, S., Sonawane, S. H., & Bhanvase, B. A. (2021). Nanomaterials for adsorption of pollutants and heavy metals: Introduction, mechanism, and challenges. In Handbook of nanomaterials for wastewater treatment (pp. 343-366). Elsevier. https://doi.org/10.1016/B978-0-12-821496-1.00032-5
30. Bokaeian, M., Fakheri, B. A., Mohasseli, T., & Saeidi, S. (2015). Antibacterial activity of silver nanoparticles produced by plantago ovata seed extract against antibiotic resistant Staphylococcus aureus. International Journal of Infection, 2(1), e22854. https://doi.org/10.17795/iji-22854.
31. Masood, R., Hussain, T., Miraftab, M., Ullah, A., Ali Raza, Z., Areeb, T., & Umar, M. (2017). Novel alginate, chitosan, and psyllium composite fiber for wound-care applications. Journal Of Industrial Textiles, 47(1), 20-37. https://doi.org/10.1177/1528083716632805.
32. Ramasamy, V., Praba, K., & Murugadoss, G. (2012). Synthesis and study of optical properties of transition metals doped ZnS nanoparticles. Spectrochimica Acta Part A: Molecular and Biomolecular Spectroscopy, 96, 963-971.https://doi.org/10.1016/j.saa.2012.07.125.
33. Iqbal, M. S., Akbar, J., Saghir, S., Karim, A., Koschella, A., Heinze, T., & Sher, M. (2011). Thermal studies of plant carbohydrate polymer hydrogels. Carbohydrate Polymers, 86(4), 1775-1783. https://doi.org/10.1016/j.carbpol.2011.07.020.
34. Rautela, A., & Rani, J. (2019). Green synthesis of silver nanoparticles from Tectona grandis seeds extract: characterization and mechanism of antimicrobial action on different microorganisms. Journal of Analytical Science and Technology, 10(1), 1-10. https://doi.org/10.1186/s40543-018-0163-z.
35. Monika, P., Chandraprabha, M. N., Rangarajan, A., Waiker, P. V., & Chidambara Murthy, K. N. (2022). Challenges in healing wound: role of complementary and alternative medicine. Frontiers in nutrition, 8, 791899. https://doi.org/10.3389/fnut.2021.791899.